

Study on Reactor Building Structure Using Ultrahigh Strength Materials  
Part 3 Cyclic Pure Shear Test of Panels

Shigeru USAMI

*Kajima Corporation, Tokyo, Japan*

Kikuo ISHIMURA

*Tokyo Electric Power Company, Tokyo, Japan*

Junichi KADORIKU

*Shimizu Corporation, Tokyo, Japan*

Haruhiko OKAMOTO

*Takenaka Corporation, Osaka, Japan*

ABSTRACT

This paper describes the structural characterizations of reinforced concrete flat panel using ultrahigh strength materials such as concrete of 98.1MPa compressive strength and rebars of 785MPa yield strength under cyclic pure shear load.

1. OBJECTIVE

The objective of research is to seek the possibility of effectively applying ultrahigh strength materials to nuclear reactor buildings. The study in this part is to comprehend the fundamental dynamic characteristics of reinforced concrete (abbr. RC) panels using ultra high strength materials by applying cyclic pure shear stress to flat panel model specimens that have no restraining members such as flange walls.

2. TEST SPECIMEN

The configuration of the test specimen is shown in Fig.1. In order to determine the level of combination of the test model, the compressive strength  $F_c$  of concrete, and the quantity  $P_s \times s_{\sigma y}$  of reinforcing steel bars (abbr. rebars) (product of rebar ratio  $P_s$  and yield strength  $s_{\sigma y}$ ) were taken into consideration, and five specimens as shown in Table 1 were selected. Three grades of concrete strength  $F_c=39.2, 68.6$  and  $98.1$ MPa and three levels of rebars quantity  $P_s \times s_{\sigma y}$  of  $4.71, 7.06$  and  $9.41$ MPa were applied. Two rebar types of SD60 and SD80 were used.

The test specimens are flat panels which are 12cm thickness, and D10 rebars of equal quantity in two directions were arranged in double layers with the concrete cover of 15mm. The mechanical properties of rebars and concrete strength used for the specimens are shown in Table 1.

3. TEST PROCEDURE

The cyclic in-plane pure shear load test was conducted by using the 'Combined Load Test System of Large Panel Element' Ref.-1 device. To apply a uniform in-plane shear load steel shear keys were used for the contact jig, and the specimen and the loading device were connected to make an integrated body. The loading hysteresis is controlled by shear strain  $\gamma$  as control

SMiRT 11 Transactions Vol. H (August 1991) Tokyo, Japan, © 1991

parameter, which is shown in Fig. 2.

The average strain of the specimens was obtained from the shear strain  $\gamma$  by a Rosette analysis of data measured from 20 transducers installed on the top and bottom surfaces of the specimen as shown in Fig. 1. Also, the average shear stress  $\bar{\tau}$  that influences the specimen was calculated from the load cell data of the loading device.

Table 1 Specimens and test results list

Items		Specimen name	#1P48L6	#2P48M6	#3P72M8	#4P72H8	#5P96H8
Specimen's values	$F_c$ (MPa)		48.5 [39.2]	82.4 [68.6]	82.4 [68.6]	101.9 [98.1]	101.9 [98.1]
	$E_c$ ( $\times 10^4$ MPa)		3.14	3.94	3.94	3.81	3.81
	$P_s$ (%)		0.79 [0.80]	0.79 [0.80]	0.92 [0.90]	0.92 [0.90]	1.18 [1.20]
	$P_s \cdot sOy$ (MPa)		4.42 [4.71]	4.42 [4.71]	7.29 [7.06]	7.29 [7.06]	9.35 [9.41]
	$sOy$ (MPa)		560 [SD60]	560 [SD60]	792 [SD80]	792 [SD80]	792 [SD80]
	$E_s$ ( $\times 10^5$ MPa)		1.95	1.95	1.93	1.93	1.93
Test results	$\tau_{cr}$ (MPa)	+Cycle	2.12	2.88	2.80	2.69	2.65
		-Cycle	-2.23	-2.89	-2.91	-2.48	-2.81
	$\tau_{cr}$	+Cycle	0.30	0.32	0.31	0.27	0.26
	$\frac{\tau_{cr}}{\sqrt{F_c}}$	-Cycle	-0.32	-0.32	-0.32	-0.25	-0.28
	$\tau_y$ (MPa)	RY	-3.84	4.92	7.55	-7.73	9.10
		RX	4.67	4.92	7.75	-7.89	8.94
	$\gamma_y$ ( $\times 10^3$ )	RY	-3.68	4.59	6.97	-7.12	7.64
		RX	5.06	4.59	7.70	-7.41	7.45
	$\tau_y$	RY	-0.87	1.11	1.04	-1.06	0.97
		RX	1.06	1.11	1.06	-1.08	0.96
	Maximum shear strength $\tau_u$ (MPa)		5.10	5.17	7.83	8.24	9.65
	$\frac{\tau_u}{P_s \cdot sOy}$		1.15	1.17	1.07	1.13	1.03
	Strain at maximum shear strain $\gamma_u$ ( $\times 10^3$ )		5.58	5.50	9.13	9.30	9.80

[ ] : Planning value or grade of rebar  
 $F_c$  : Concrete compressive strength  
 $E_c, E_s$  : Young's modulus of concrete and rebar  
 $sOy$  : Rebar yield strength  
 $\tau_y$  : Shear stress at rebar yield  
 $\tau_u$  : Maximum shear strength  
 $RY$  : Y-directional rebar  
 $\tau_{cr}$  : Shear cracking stress  
 $\gamma_y$  : Shear strain at rebar yield  
 $\gamma_u$  : Shear strain at maximum strength  
 $RX$  : X-directional rebar

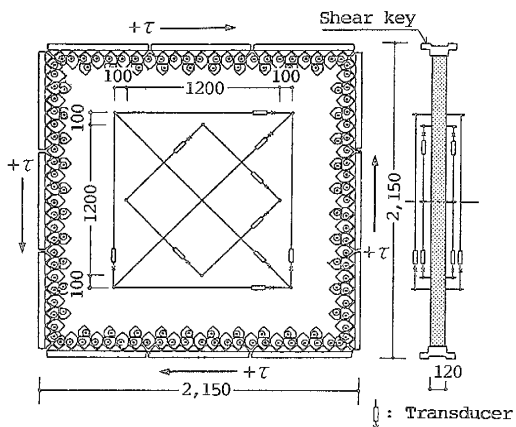


Fig. 1 Specimen shape and measuring points

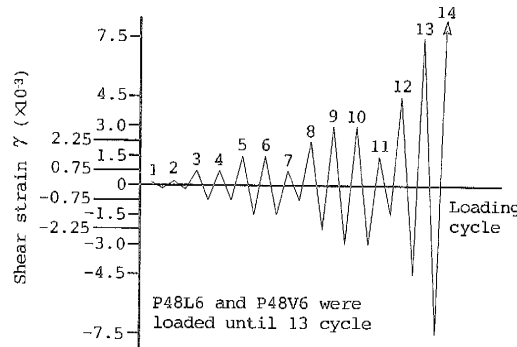


Fig. 2 Loading schedule

#### 4. TEST RESULTS

##### 4.1 Outline

The results of the various specimens are shown in Table 1. The rebar yield shown in Table 1 is defined as the rebar yield strain in any one of the gage of rebars when it reached the yield strain obtained by material test.

The shear strain value at maximum strength is the value when it was initially attained regardless of its continuation. Shown in Fig. 3 is the relation of shear stress-shear strain, in Fig. 4 is typical example of cracking, and in Fig. 5 is typical example of strain distribution of the rebars. From these figures the following was learned:

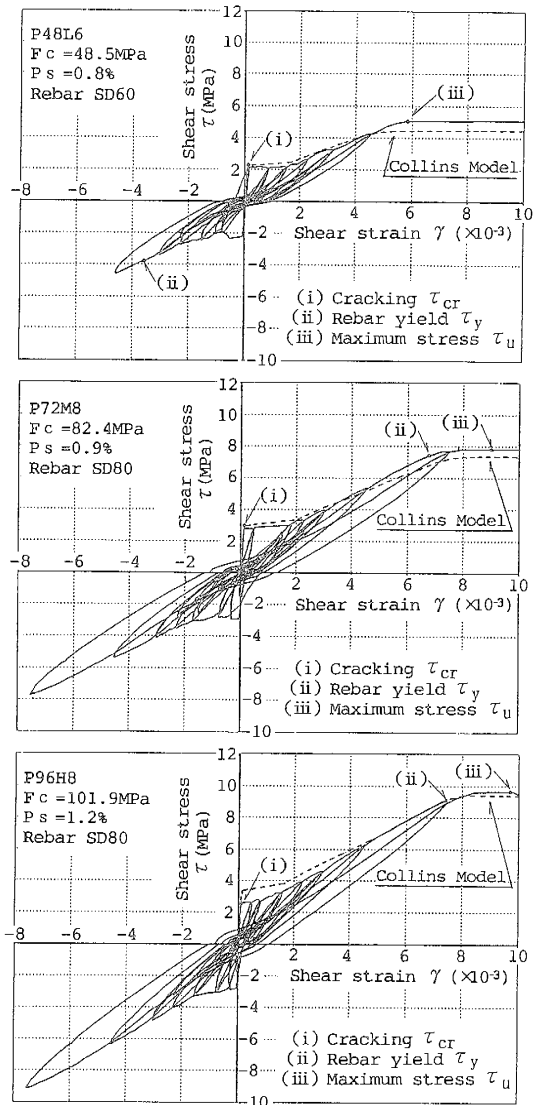


Fig. 3 Relation of shear stress versus shear strain

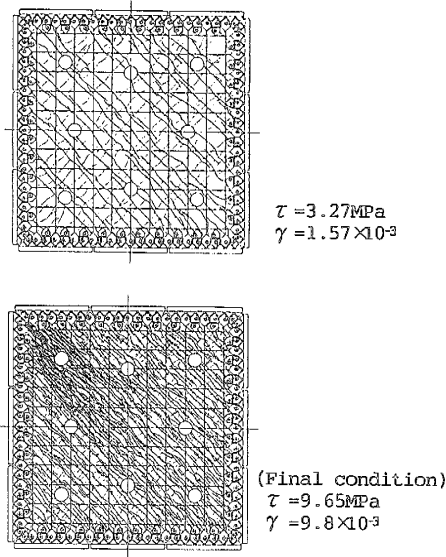


Fig. 4 Cracking conditions (P96H8)

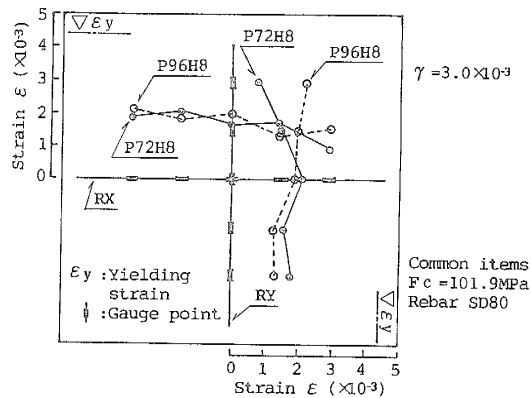


Fig. 5 Rebar strain distribution (P72H8 & P96H8)

- (1) All of the specimens showed that when the initial shear crack was induced, the shear strain increased suddenly. The distinction at this time was that there was no stress increase. Also, as the specimens had been selected so that the maximum strength could be determined with the rebar yield, all of them followed the course of attaining maximum strength after the rebar yield. The maximum shear stress  $\tau_u$  is 1.1 times rebar yield  $\tau_y$ . Meanwhile, shear strain  $\gamma_u$  at the time of  $\tau_u$  showed  $5.5$  to  $9.8 \times 10^{-3}$  which is a large strain value when compared with the conventional normal walls.
- (2) For all test specimens the number of cracks increased with the increase of shear strain  $\gamma$ . At the time of final demolition the cracks expanded while converging in the approximate diagonal direction of the specimen, and the rebars at that portion ruptured that led to ultimate failure.
- (3) Regarding the distribution of rebar strain, in case of SD80 with concrete of class 98.1MPa, even when the shear strain is quite large such as  $\gamma=3.0 \times 10^{-3}$ , not much difference was noticed due to the rebar quantity ( $P_s \times s \sigma_y$ ).
- (4) Also shown in Fig. 3 is the  $\tau$ - $\gamma$  of experimental result as compared with analysis value by Collins model Ref.-2. The analysis value  $\tau_u$  is evaluated somewhat smaller than the experimental result, however, it can be said that the general analysis value is in good compliance with the test results.

#### 4.2 Relation of $\tau$ - $\gamma$

The enveloped graphic lines of  $\tau$ - $\gamma$  relation is shown in Fig. 6. In this figure the difference by concrete compression strength  $F_c$  only is shown. In other words, a difference in  $\tau$ - $\gamma$  between the test specimen #1 (to be called #1 through #5) of  $F_c=48.5$ MPa (unit omitted hereafter), and #2 of  $F_c=82.4$  is noticed. It is found that at the 2nd gradient ( $\tau$ - $\gamma$  relation from start of cracks to yield) the larger  $F_c$  has larger shear stress at the same deformation. Also, at the larger level of  $F_c$ , between #3 of  $F_c=82.4$  and #4 of  $F_c=101.9$ , when the  $\tau$ - $\gamma$  was compared, no difference was found between the two. Next, regarding the comparison of  $\tau$ - $\gamma$  between #4 of  $P_s \times s \sigma_y = 7.06$ MPa (unit omitted hereafter) and #5 of  $P_s \times s \sigma_y = 9.41$ , it can be said that the specimens with the larger  $P_s \times s \sigma_y$  had the larger shear stress at the 2nd gradient and at maximum strength.

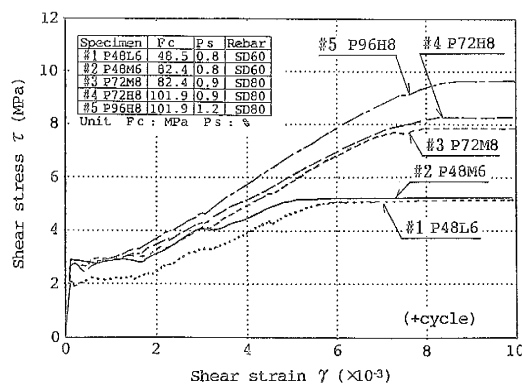


Fig. 6 Relations of shear stress versus shear strain

#### 4.3 Condition of cracks

The relation of cracks outbreak shear stress  $\tau_{cr}$  and the concrete compression strength  $F_c$  is shown in Fig. 7. Also, shown together in the figure are the test results of Ref.-3. From this figure, it is noted that as  $F_c=48.5$  #1 increases to  $F_c=82.4$  #2,  $\tau_{cr}$  increases in relation with  $0.313\sqrt{F_c}$ . Moreover, when  $F_c$  increased to  $F_c=101.9$  #4 and #5,  $\tau_{cr}$  shows no increase indicating that the relation of  $F_c$  and  $\tau_{cr}$  has marked the ceiling. In case that Ref.-3 is included,  $0.313\sqrt{F_c}$  indicates about the upper limit of  $\tau_{cr}$ .

#### 4.4 Maximum strength

The relation of the tests of maximum shear strength  $\tau_u$  and the calculated value  $P_s \times s \sigma_y$  is shown in Fig. 8. Also, shown together is the test results of Ref.-3. From this figure it is noted that when  $\tau_u$  is determined by rebars then  $\tau_u$  value can be evaluated by  $P_s \times s \sigma_y$  as the same as RC panels with normal material strength. Also, it can be seen that by comparison of  $F_c=48.5$  #1 with  $F_c=82.4$  #2, and  $F_c=82.4$  #3 with  $F_c=101.9$  #4, if  $P_s \times s \sigma_y$  are the same, then when  $F_c$  increases  $\tau_u$  slightly increases.

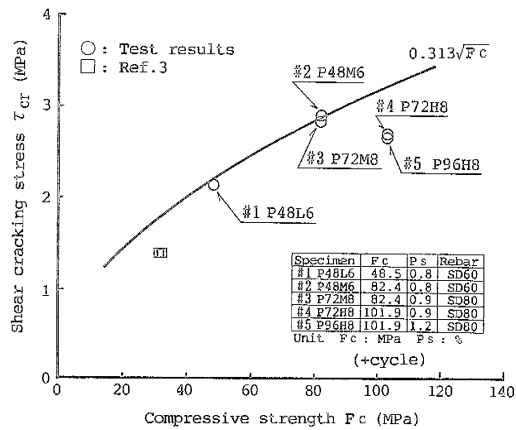


Fig. 7 Shear cracking stress versus concrete compressive strength

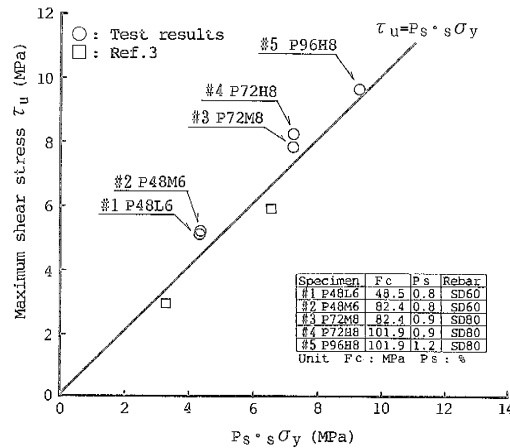


Fig. 8 Relation of maximum shear stress versus  $P_s \cdot s \cdot \sigma_y$

#### 4.5 Restoring force characteristics

(1) Residual strain divided by peak strain is defined as  $\beta$ , and the relation of  $\beta$  and peak strain  $\gamma$  is shown in Fig. 9. Also, in this figure,  $\beta$  at time of initial loading is connected by a line and  $\beta$  at the time of repeated loading is shown by dott. This figure shows that for all of the specimens when  $\gamma$  increases  $\beta$  becomes smaller, or in other words, the restoration is excellent. At  $\gamma=4.0 \times 10^{-3}$  and beyond it, with no relation to  $F_c$  and  $P_s \times s \sigma_y$ ,  $\beta$  is concentrated at approximately 0.2. Also,  $\beta$  at time of repeated loading (dott in the figure) is small when compared with  $\beta$  of initial loading time (line in the figure).

(2) The relation of equivalent viscous damping factor  $h_e$  and  $\gamma$  is shown in Fig. 10. From this figure it can be seen that with all of the specimens with the increase of  $\gamma$ , with no relation to  $F_c$  and  $P_s \times s \sigma_y$ , the value of  $h_e$  becomes small and at more than  $\gamma=4.0 \times 10^{-3}$  it converges to approximately 0.05.

The value of  $h_e$  at time of repeated loading under same deformation becomes small when compared with the time of initial loading but its value is 0.045 at minimum which is about equivalent with the average value 0.046 of repeated loop relevant with the research of shear wall described in Ref.-5.

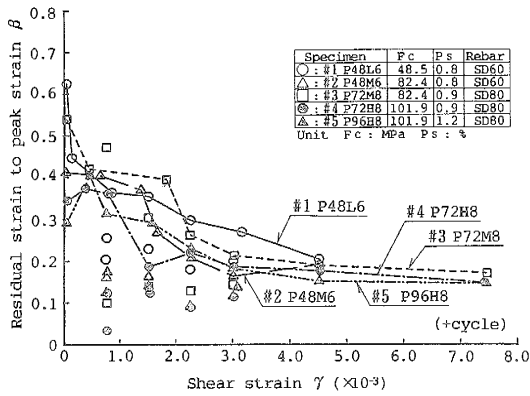


Fig. 9 Relation of residual strain to peak strain versus shear strain

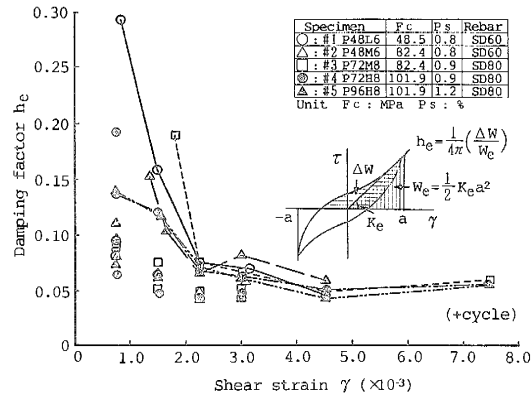


Fig. 10 Relation of equivalent damping factor versus shear strain

## 5. CONCLUSION

In the outline of this report the characteristics of RC panels subjected to pure shear when ultrahigh strength materials (e.g. concrete strength 98.1MPa and rebar SD80) were used were learned. And in the latter part of this report it was learned that ; i) When  $F_c$  and  $P_s \times s \sigma_y$  becomes large, the maximum strength and stress of 2nd gradient of  $\tau$ - $\gamma$  relation envelope line increases ; ii) In case that  $F_c$  is smaller than 82.4MPa, shear crack outbreak stress can be evaluated approximately by  $0.313\sqrt{F_c}$  ; iii) When  $\tau_u$  is determined by rebars, the maximum strength can be evaluated generally by  $P_s \times s \sigma_y$  ; iv) Residual strain divided by peak strain converges to about 0.2 at  $\gamma = 4.0 \times 10^{-3}$  and beyond it; v) Equivalent viscous damping factor was 0.045 at least at repeated loops.

## REFERENCES

1. Kurihara K. and et al. (1984). Experimental Investigation on Reinforced Concrete Panels Subjected to Combined Membrane Stresses Part 1, Proc. of the Annual Congress of AIJ, pp.1801-1802
2. Vecchio F.J. and Collins M.P. (1982). Response of Reinforced Concrete to In-Plane Shear and Normal Stresses, Publication 83-03, University of Toronto
3. Kusama K. and et al. (1985). Experimental Investigation on Reinforced Concrete Panels for RCCV under In-Plane Shear Loading, Proc. of the Annual Congress of AIJ, pp.817-818
4. Matumura T., Kodama J. and et al. Allowable Limit of Shear walls of Reactor Buildings Part 1,2, Proc. of the Annual Congress of AIJ, 181-184,
5. Inada Y. (1989). Load-Displacement Relationship of Reactor Buildings Subjected to Earthquake Forces, Special Report of Ins. of Tech., Shimizu Corp. No.27